DISASTER SCIENCE AND ENGINEERING p. 67-75, 2(2), 2016

Seismic Behaviour Evaluation of Suleymaniye Mosque Under Different Earthquake Records

Ayhan Aslan, Abdurrahman Sahin

Received: 25.04.2016 Accepted: 05.06.2016

Abstract In this study, 3D structural model of Suleymaniye Mosque which Mimar Sinan began the construction in 1550 and finished in 7 years is developed and the behavior is examined under the influence of different earthquakes. Finite element (FE) model of the structure is generated and modal analysis is carried out. The obtained dynamic characteristics such as natural frequencies and mode shapes are compared with experimental works and the FE model is updated. Earthquake analysis of the mosque is carried out by using actual earthquake records of the past. The structural behavior under the earthquake effects is obtained at the end of the analyses and the most affected areas of the structure have been determined. The results are evaluated and comments are made about the structure.

***Index Terms*—Suleymaniye Mosque, Earthquake Analysis, Historical, Masonry Structures, Finite Element Method, Sap2000**

I. Introduction

Modeling a complex structure such as Suleymaniye Mosque is extremely difficult. Modeling should be done by making some assumptions and idealizations. Assumptions are made for uncertain data such as material properties and other parameters which are difficult to determine with test or observation. Macro modeling approach may be chosen for this kind of huge and complex structures. In this approach, the structural system is modeled with continuous structural element such as solid or shell. The structural analysis is carried out and the obtained results are evaluated.

II. General Knowledge About Suleymaniye Mosque

A. Location of the Structure

Suleymaniye Mosque, is located in Fatih District of Istanbul. The geodetic position of the structure is 28°57′50″ deg longitude and 41°00′58″ deg latitude as shown in Fig. 1. At that area, outcropping bedrock may be observed and the structure was settled on very stiff soil.

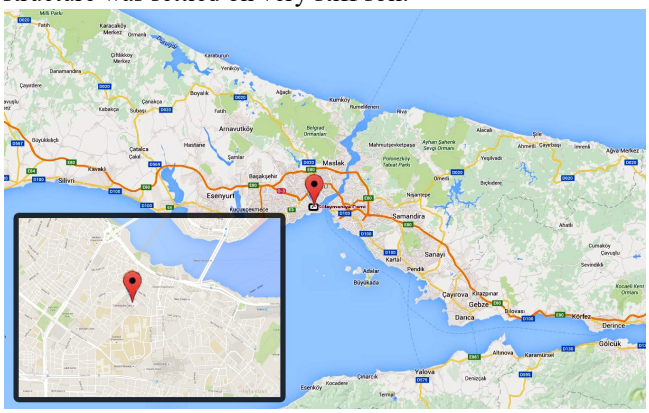

Fig. 1. Location of Suleymaniye Mosque [1]

B. Structural Properties of Suleymaniye Mosque

Suleymaniye Mosque was built on the four pillars each is calculated as approximately 30 tons. The main dome and the upper masonry shell transfer about 1000t load to the base with two half domes and piers. It is thought that each pillar transfers 8000 t loads to the base. There are four main arches between the piers [2].

Main dome of the mosque stands on pillars and main arch. The dome of the mosque is 50.5-meter-high and its diameter is 27.5 meters. There are 32 windows in the dome rim. Two half-dome supports the main dome from sides. These half-domes are also supported by two smaller domes. Five domes

This study is prepared from the paper presented in International Symposium on Natural Hazards and Hazard Management 2016.

Ayhan ASLAN is with the Civil Engineering Department, Yıldız Technical University (e-mail: ayhan-aslan@yandex.com).

Abdurrahman SAHIN is with the Civil Engineering Department, Yıldız Technical University (e-mail: abdsahin@yildiz.edu.tr).

are available in various sizes on locations where there is not any half dome. Further, there are twenty-eight small domes in the courtyard.

Fig. 2. Suleymaniye Mosque [3]

There are four minarets on mosque as shown in Fig. 2. The reason is that Suleyman the Magnificent is the fourth Ottoman Sultan after the conquest of Istanbul. These minarets are located in the four corners of the courtyard. The minarets which are adjacent with the mosque (Eastern and southern minarets) are 76 meters high, and have three balconies. The minarets which are not adjacent with the mosque (Northern and western minarets) are 55 meters high, and have two balconies. The ten balconies on the four minarets are symbol that Suleyman the Magnificent is the tenth sultan of the Ottoman Empire.

It is observed that Suleymaniye Mosque settled on outcropping bedrock. It can be said that the site of the mosque has high compressive strength compared to many other locations in Istanbul [4].

Suleymaniye Mosque which is the main building of the Suleymaniye Complex is 114.88 m long along the Kaaba axes with courtyard, 64.68 m without the courtyard. In the perpendicular direction, it is 69.23 m.

The mosque is built on a total area of 7046.5 m2; including the courtyard is 3049 m2. The total circumference of the mosque outline is 339.5 m. The total perimeter of the courtyard outline is 230.4 m. The total circumference of the whole system is 444.9 m. The mosque is almost completely symmetrical along the Kaaba axis and close to symmetrical perpendicular to Kaaba axis. (Fig.3) [5].

III. Structural Model And Analysis

The material properties and model types used in structural model are presented in Table 1. The material properties used here are obtained from previous study made by Dabanlı [6] and updated depending on the experimental test results carried out by Selahiye et al. [7]. After material properties are updated, a good harmony is observed between analytical natural frequencies and experimental natural frequencies.

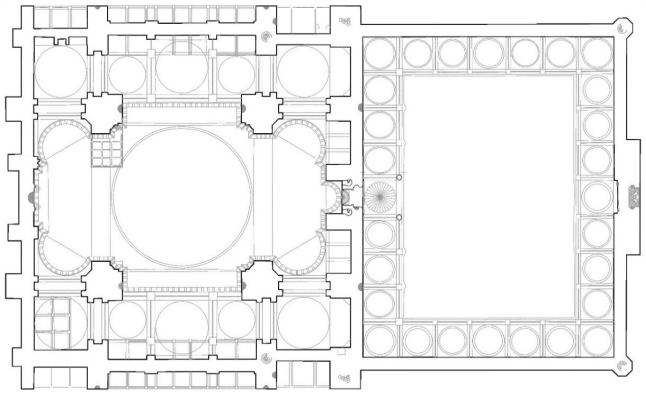

Fig. 3. Plan View of the Mosque [5]

TABLE I
MATERIAL PROPERTIES USED IN THE MODEL

Structural Element	Element Type	Model Type	Modulus Of Elasticity (MPa)	Density (Kg/M3)	Poisson Ratio
Walls	Stone	Solid	9500	2200	0,2
Minarets	Stone	Solid	9500	2200	0,2
Domes	Brick	Shell	3000	1800	0,18

IV. Finite Element Model

The Finite Element (FE) model of Suleymaniye Mosque has been constructed with Sap2000 commercial software. In modeling process, guide lines have been imported into Sap2000 through AutoCAD. The detailed modeling stages are presented in Fig. 4. The model contains 48172 points, 2658 shell elements and 23500 solid elements. The model is located in an area which is 114.08 m in X axis, 69.13 m in Y axis and 73.25 m in Z axis. The end ornaments at the top of the minarets are neglected in model because they are not effective on the structural behavior.

V. Dynamic Analysis

Modal analysis is performed to determine the natural frequencies and mode shapes of the structure. The modal vectors are determined depending on the maximum mass participation ratios as shown in Table 2.

As a result of modal analysis of the structure, the first 100 mode is considered and it is seen that total mass participation ratio is 77.12% in X direction and 77.16% in Y direction. It is seen that 14th mode shape has the maximum mass participation ratio in X direction with 54.17% and 15th mode shape has the maximum mass participation ratio in Y direction with 40.91%. The modes with maximum mass participation ratios are given in Table 2. The mode shapes of the structure are presented in Figs. 5-8. As it can be seen from these Figures, the first mode is translation in X direction, the second mode is translation in Y direction, the third mode is rotation about Z direction and the fourth mode is translation in Z direction. The increase in mass participation ratio is very limited from 68th mode, so that total 100 mode is taken into

account in this study.

TABLE II
MODAL MASS PARTICIPATION RATIOS

Mode Number	UX (%)	UY (%)	UZ (%)	RZ (%)
Mode 14	**54,17**	0,526	5,2 E-7	0,003
Mode 15	0,749	**40,912**	1,4 E-4	4,559
Mode 16	0,052	0,154	8,4 E-4	**12,09**
Mode 66	0,032	0,051	**5,026**	0,083

The natural frequency values which corresponds the determined mode shapes are compared with previous experimental and analytical studies as given in Table 3. As it can be seen from this table, there is a good harmony between the current study and previous studies.

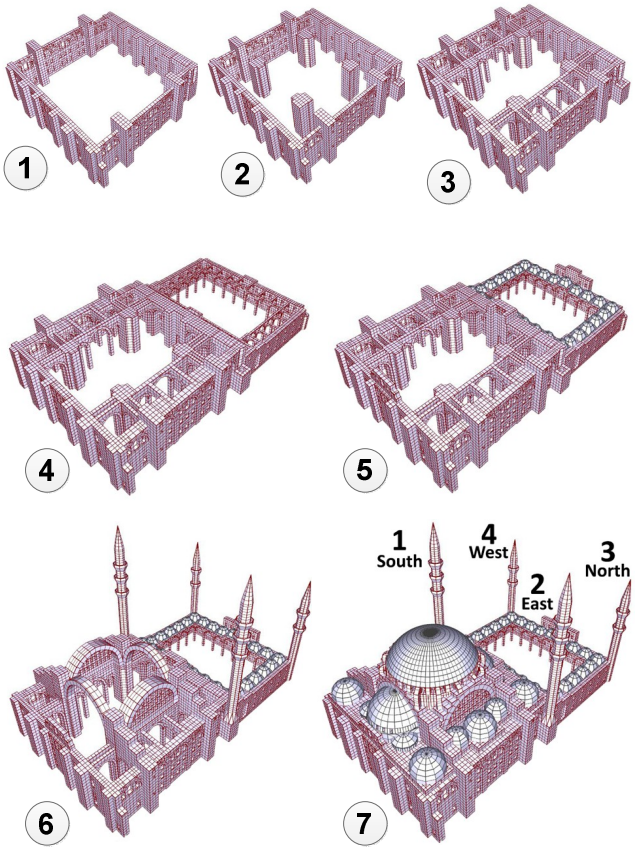

Fig. 4. Modeling stages of Suleymaniye Mosque

Three earthquake records are selected and applied to the structure. The acceleration records are given in Figs. 9-11 and the displacement records are given in Figs. 12-14. Time history analyses are carried out and the obtained results are evaluated. The East-West components of earthquake records are applied in X direction of the structure and North-South components of earthquake records are applied in Y direction of the structure. Tensile and compressive stress distribution over the structure from static analysis is given in Table 4. The maximum stress distribution in the structure from earthquake analyses is given in Table 5 and 6. Displacement distribution observed in some critical parts of the structure is also given in Table 7.

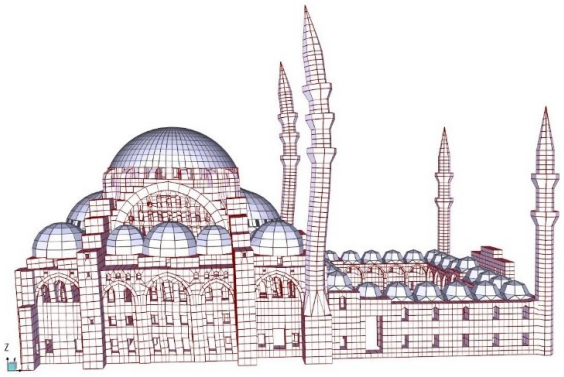

Fig. 5. First mode shape (translation in X direction)

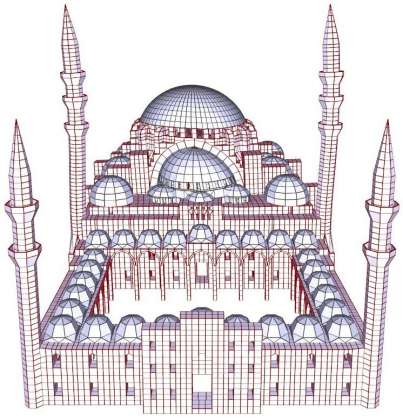

Fig. 6. Second mode shape (translation in Y direction)

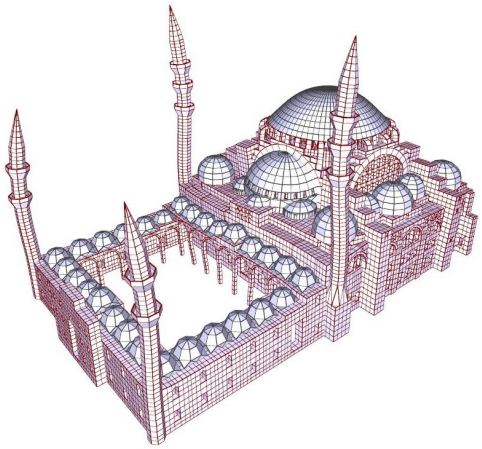

Fig. 7. Third mode shape (rotation about Z direction - torsion)

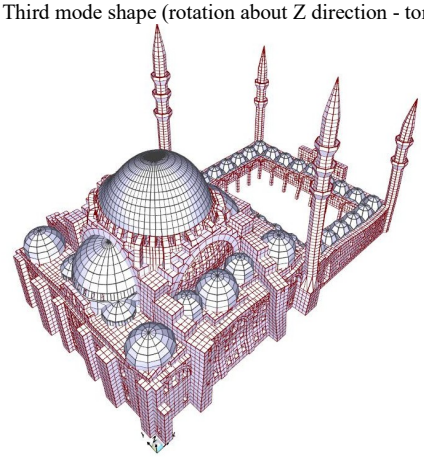

Fig. 8. Fourth mode shape (translation in Z direction)

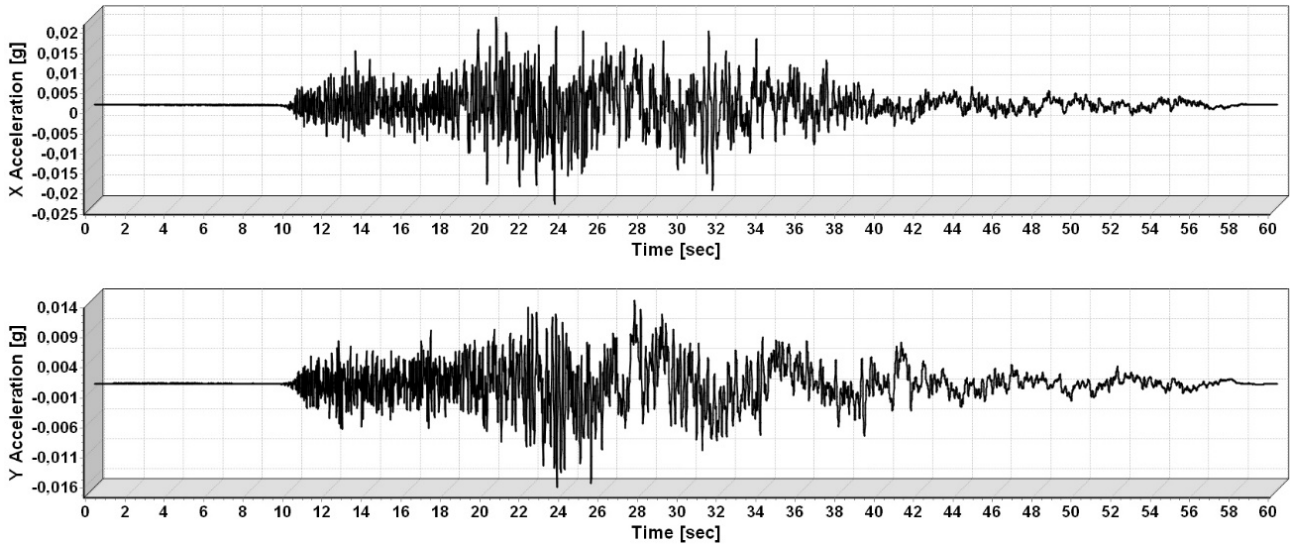

Fig. 9. Düzce Earthquake (1999) acceleration record from Sakarya Station [8, 9]

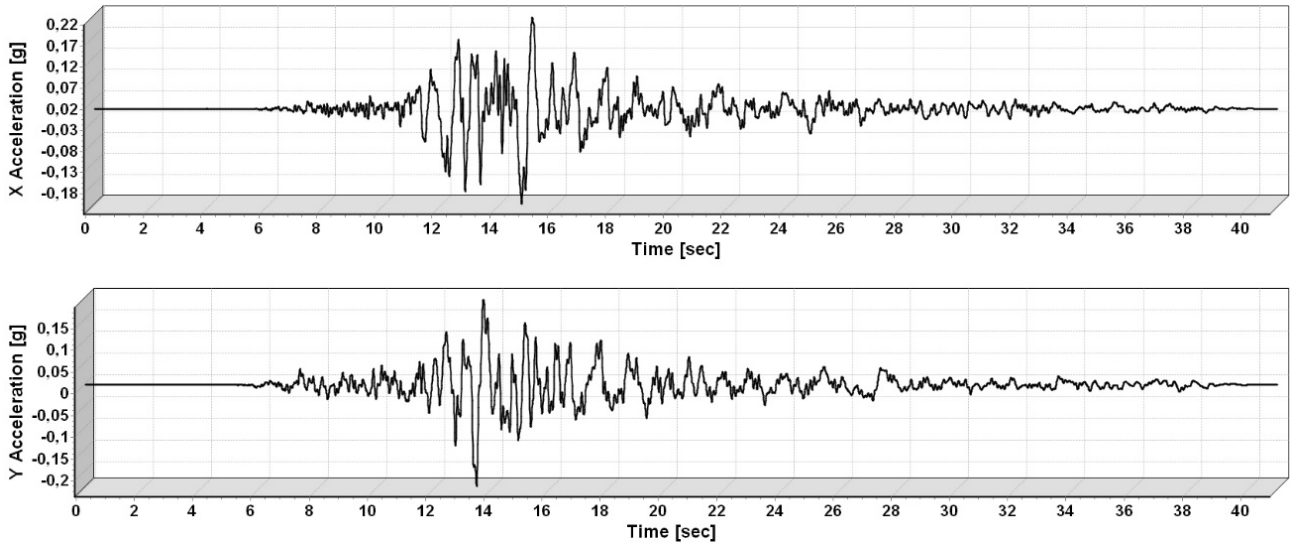

Fig. 10. Kobe Earthquake (1995) acceleration record from Shin-Osaka Station [8, 9]

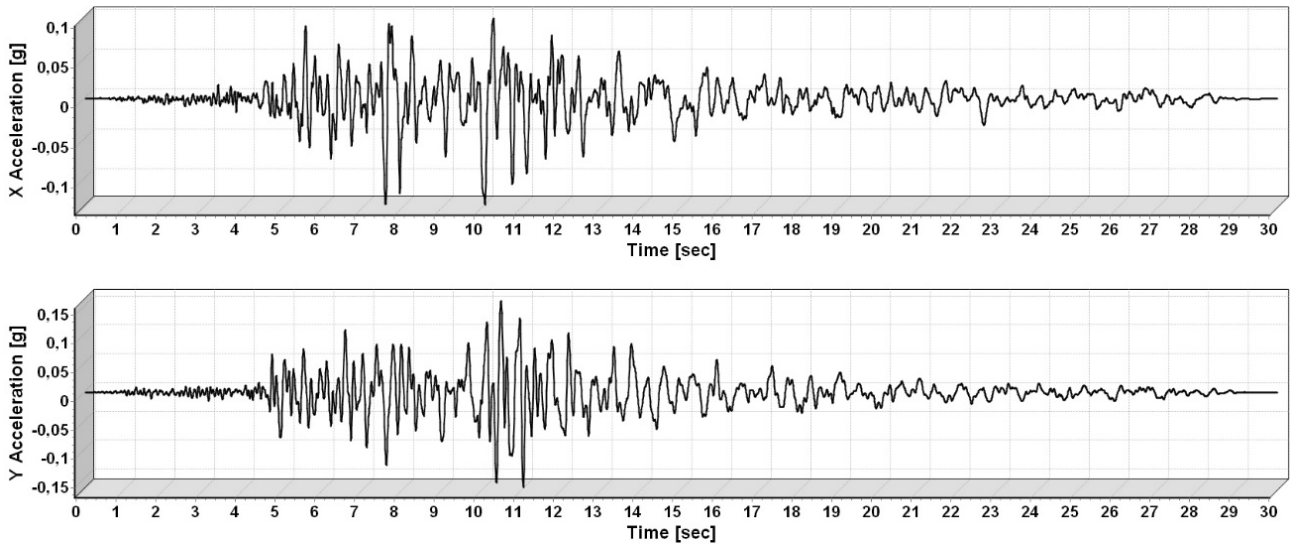

Fig. 11. Northridge Earthquake (1994) acceleration record from LA - N Figueroa Station [8, 9]

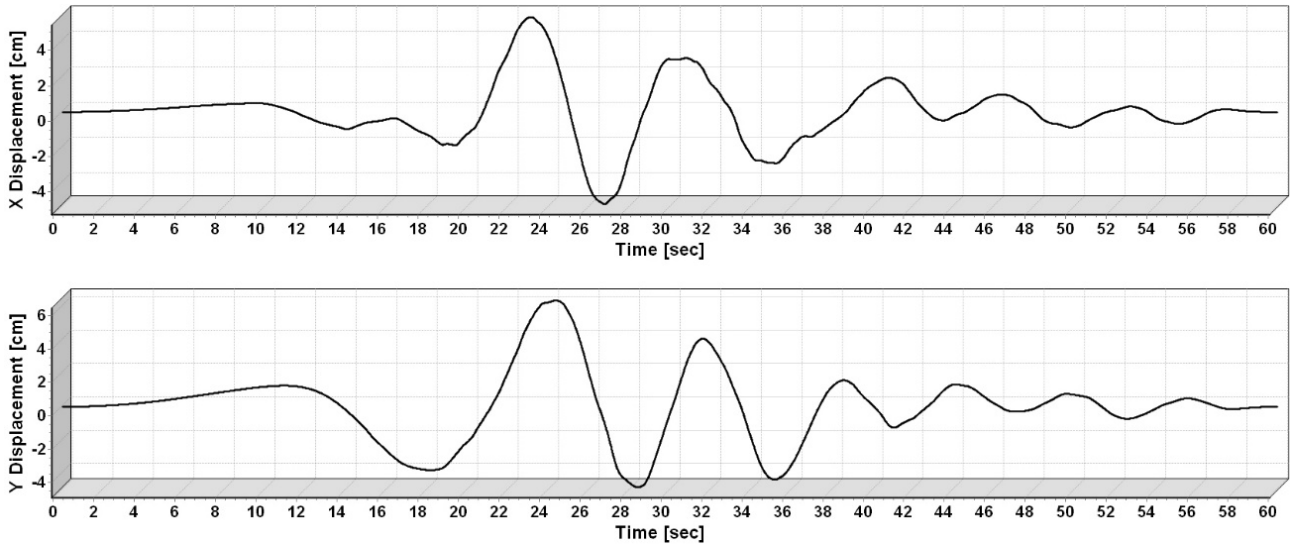

Fig. 12. Düzce Earthquake (1999) displacement record from Sakarya Station [8, 9]

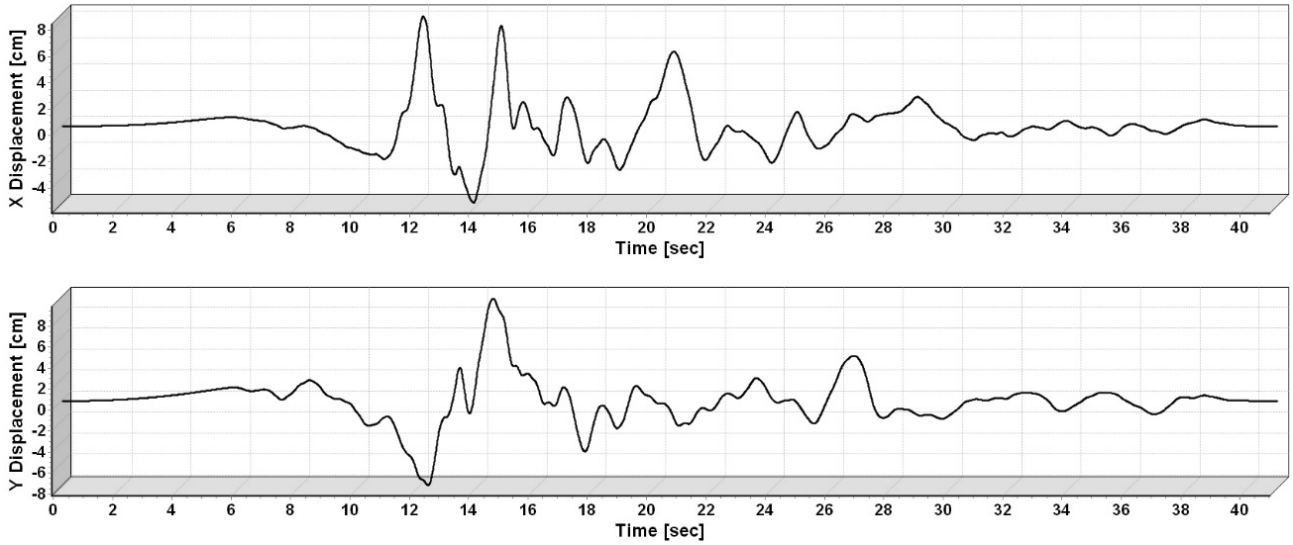

Fig. 13. Kobe Earthquake (1995) displacement record from Shin-Osaka Station [8, 9]

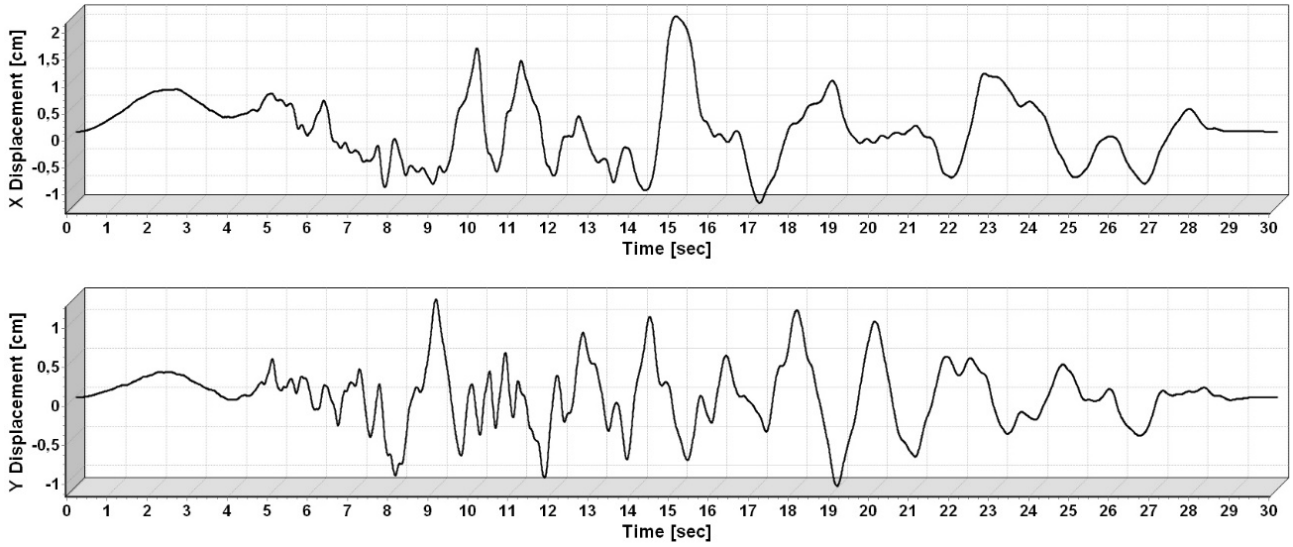

Fig. 14. Northridge Earthquake (1994) displacement record from LA - N Figueroa Station [8, 9]

TABLE III
COMPARISON OF OBTAINED FREQUENCIES WITH PREVIOUS WORKS

Mode No	Analytical Frequencies by Aslan and Sahin (Hz)	Experimental Frequencies by Selahıye et al. [7] (Hz)	Experimental Frequencies by Sato et. al. (Hz) [10]		Analytical Frequencies by Seker (Hz) [11]
			Before Kocaeli Earthquake	After Kocaeli Earthquake	
Mode 14	3,366	3,38	3,43	3,36	4,07
Mode 15	3,486	3,44	3,55	3,46	4,75
Mode 16	4,247	4,26	-	-	-
Mode 66	9,013	9,60	-	-	-

VI. Conclusion

The maximum compressive stress from static analysis in vertical direction (S33) is 2.35 MPa as shown in Table 4. The compression stress distribution over the structure through Z axis from static analysis is given in Fig. 15. The graphics presented in this study are scaled between -1Mpa and 1 MPa for better evaluation of the stress distribution. It can be seen that the structure is very heavy. Also it is seen that tensile stresses may also occur in the structure due to the dead weight. The maximum tensile stress in Y direction (S22) due to its own weight is 1.31 MPa.

TABLE IV
TENSILE AND COMPRESSIVE STRESS DISTRIBUTION OVER THE STRUCTURE FROM STATIC ANALYSIS.

	SHELL ELEMENTS		SOLID ELEMENTS		
	S11	S22	S11	S22	S33
TENSILE STRESS	0,68	0,69	1,06	1,31	1,22
COMPRESSION STRESS	1,22	1,52	1,25	2,03	2,35

The maximum compression and tensile stresses due to earthquake effects are given in Tables 5 and 6. The maximum tensile stresses are obtained due to Kobe earthquake applied in X direction. The stress distribution due to this record is presented in Fig. 16. The most parts of the structure are under the tensile effects lower than 1 MPa. Tensile stresses around 3 MPa are observed on walls of the minarets and tensile stresses around 1.5 MPa are observed near window openings.

As shown in Fig. 17, tensile stresses between 1 MPa and 2 MPa are observed near the base of the structure. The maximum tensile stress distribution due to Y component of Kobe earthquake is presented in Fig. 18.

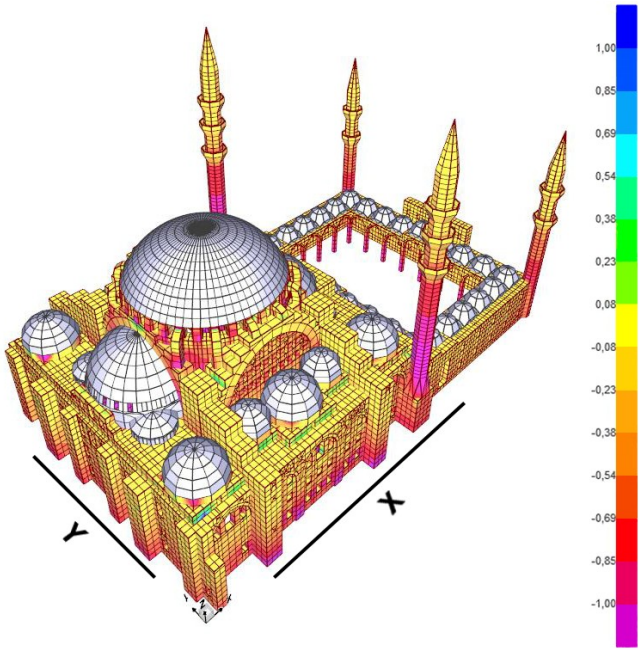

Fig. 15. Compression stress distribution over the structure through Z axis due to its own (S33)

TABLE V
MAXIMUM TENSILE STRESSES DUE TO EARTHQUAKE EFFECTS (MPa)

MAX. TENSILE STRESSES	SHELL		SOLID		
	S11	S22	S11	S22	S33
Düzce (X)	0,75	0,89	1,3	**1,91**	1,37
Düzce (Y)	0,72	0,73	1,24	**1,62**	1,35
Kobe (X)	1,34	1,85	4,09	3,18	**5,76**
Kobe (Y)	2,18	2,07	2,56	3,25	**5,34**
Northridge (X)	1,13	1,53	3,26	2,58	**3,87**
Northridge (Y)	1,79	1,22	1,96	**3,52**	3,14

TABLE VI
MAXIMUM COMPRESSION STRESSES DUE TO EARTHQUAKE EFFECTS (MPa)

MAX. COMPRESSION STRESSES	SHELL		SOLID		
	S11	S22	S11	S22	S33
Düzce (X)	1,4	1,65	1,79	2,15	**2,94**
Düzce (Y)	1,43	1,59	1,37	2,09	**2,99**
Kobe (X)	2,32	2,44	4,16	3,35	**6,97**
Kobe (Y)	2,49	2,53	2,29	3,64	**6,45**
Northridge (X)	2,1	2,13	4,19	2,93	**4,84**
Northridge (Y)	2,06	2,22	2,17	3,78	**4,45**

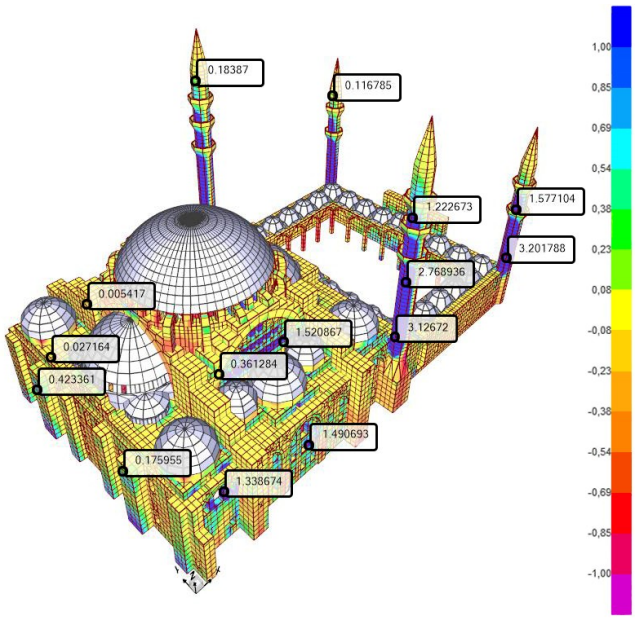

Fig. 16. Maximum tensile stress distribution through Kobe earthquake in X direction (Table 5, S11).

Similar to Kobe earthquake, the largest tensile stress are observed in X components of Duzce and Northridge earthquakes. The largest stresses in Y direction are observed due to Kobe earthquake. The details of tensile stress distribution over the south minaret surface due to X component of Kobe earthquake is presented in Fig. 19. The details of compression stress distribution over the north minaret surface due to Y component of Kobe earthquake is presented in Fig. 20.

The increase in tensile stress increases the probability of crack occurrence over the structure. The maximum crack formation may be expected due to Kobe earthquake.

The greatest pressure effects are observed in vertical direction (S33) due to all earthquake records because the structure is too heavy.

In the domes, maximum pressure is observed where they connect with other domes or main structure as shown in Fig. 21. The maximum tensile stresses are observed at the places where the maximum compression stresses are observed. The tensile stress distribution over the domes due to Y component of Northridge earthquake is given in Fig. 22. It can be said that the compressive and tensile stresses observed over the domes are lower compared to main structure.

As it can be seen from Table 7, the structure is not affected seriously due to Duzce earthquake and the displacements are very limited. The behavior of the main structural system is very rigid and the displacements are limited. The maximum displacements are observed at the top joints of south and east minarets. The maximum displacement value of top joints of minarets is 251 mm under the X component of Kobe earthquake.

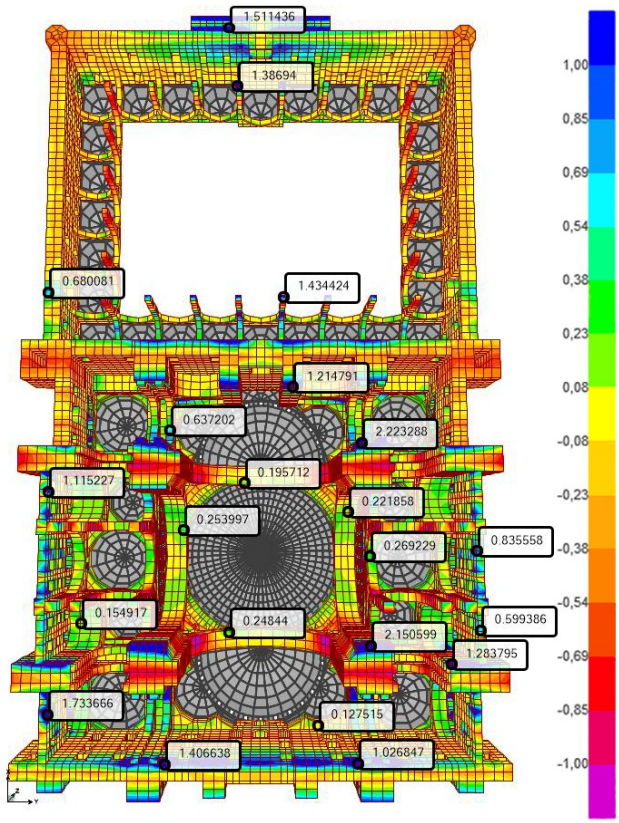

Fig. 17. Tensile stresses in vertical direction due to X component of Kobe earthquake (Table 5, S33).

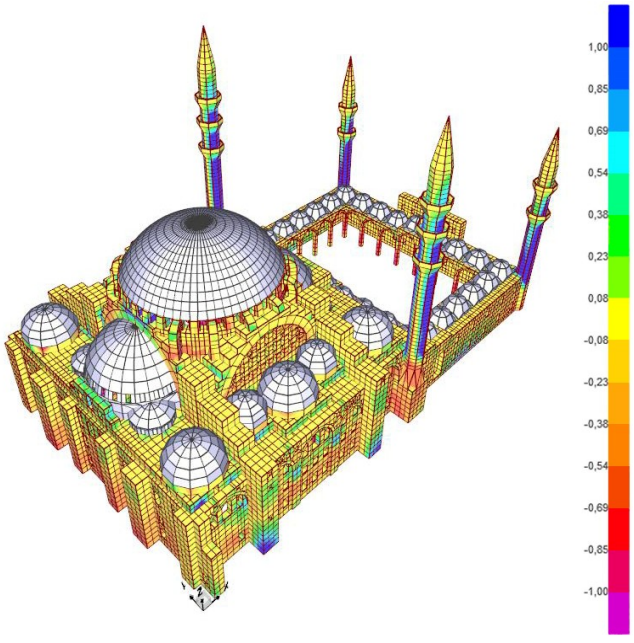

Fig. 18. Maximum Tensile stress distribution due to Y component of Kobe earthquake (Table 5, S22).

TABLE VII
MAXIMUM DISPLACEMENTS AT TOP JOINTS OF THE STRUCTURE DUE TO DIFFERENT EARTHQUAKE EFFECTS

Top Joint	Düzce earthquake (mm)				Kobe earthquake (mm)				Northridge earthquake (mm)			
	Max (X)	Min (X)	Max (Y)	Min (Y)	Max (X)	Min (X)	Max (Y)	Min (Y)	Max (X)	Min (X)	Max (Y)	Min (Y)
Big Dome	1,87	-1,97	1,03	-0,99	9,53	-13,83	9,97	-9,64	7,13	-9,64	8,38	-9,12
(1) South Minaret	9,48	-20,1	14,23	-22,9	251,6	-217,7	146,4	-182,8	46,79	-88,3	46,57	-106,9
(2) East Minaret	9,25	-19,6	14,11	-23	251,2	-226,5	147,7	-178,9	45,33	-87,8	45,61	-104
(3) North Minaret	15,79	-16,1	15,34	-19,6	203,1	-188,4	178,2	-189,2	74,78	-81,9	39,36	-43,84
(4) West Minaret	15,83	-16,2	15,39	-19,6	202,5	-187,1	178,5	-190,1	74,69	-81,6	39,3	-43,99

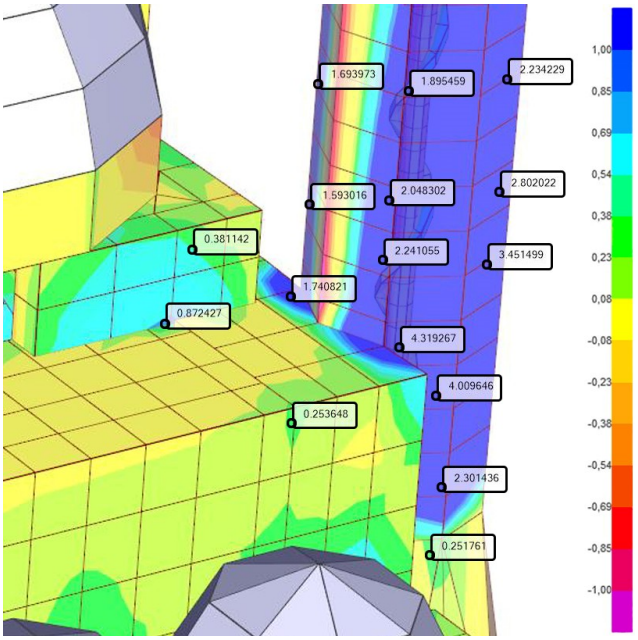

Fig. 19. Tensile stresses over the surface of south minaret due to X component of Kobe earthquake (Table 5, S33).

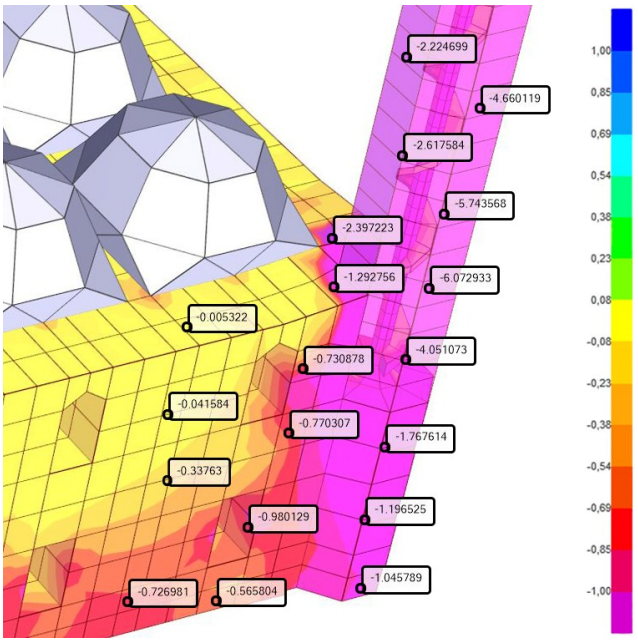

Fig. 20. Compression stresses over the surface of north minaret due to Y component of Kobe earthquake (Table 6, S33).

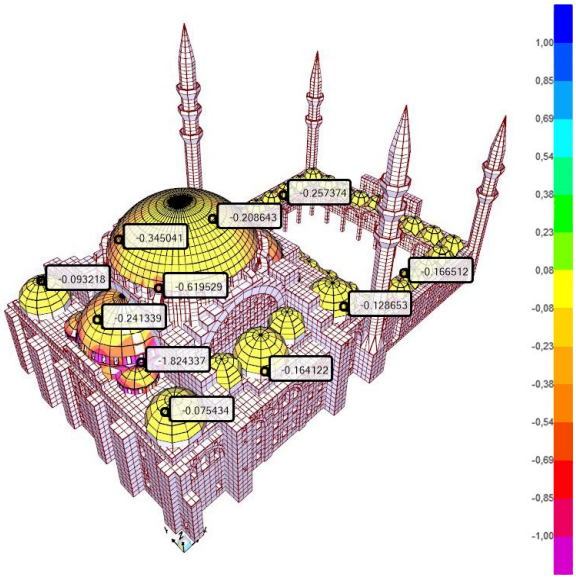

Fig. 21. Maximum compression stresses over the domes due to Y component of Northridge earthquake (Table 6, S11).

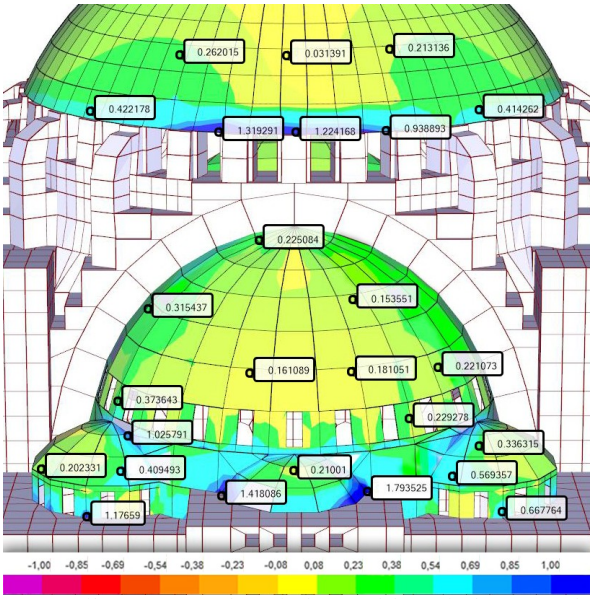

Fig. 22, Tensile stresses over the main dome and domes in the courtyard side due to Y component of Northridge earthquake (Table 5, S11).

REFERENCES

[1] Google Maps, [Online]. Available: maps.google.com.

[2] Kubbe (Kemer, Ayak ve Sütunlar), [Online]. Available: www.suleymaniyecamii.org. (in Turkish)

[3] https://youtu.be/9H-AGb2U27A. Taken from video, Kubbe-i Mina, December 2015.

[4] F. ÇILI, O. C. ÇELİK ve H. SESİGÜR, "Süleymaniye Camii Taşıyıcı Sisteminin Onarımı Ve Güçlendirme Çalışmaları", *Vakıf Restorasyon Yıllığı,* no. 3, 2011. (in Turkish)

[5] T.R. Prime Ministry Directorate General of Foundations, Suleymaniye Mosque structure survey, January 2007.

[6] Ö. DABANLI, "Tarihi Yığma Yapıların Deprem Performansının Belirlenmesi", Yüksek Lisans Tezi, İstanbul: İstanbul Teknik Üniversitesi, Fen Bilimleri Enstitüsü, Haziran 2008. (in Turkish)

[7] A. SELAHİYE, M. N. AYDINOĞLU ve M. ERDİK, "Süleymaniye Camii'nin dinamik özelliklerinin deneysel ve analitik yöntemler ile belirlenmesi", *Üçüncü Ulusal deprem Mühendisliği Konferansı*, İstanbul, Mart 1995. (in Turkish)

[8] *PEER Ground Motion Database,* [Online]. Available: *ngawest2.berkeley.edu,* University of California, 2015.

[9] *SeismoSignal,* Pavia, Italy.: Seismosoft Ltd., 2013.

[10] T. Sato, Y. Nakamura and J. Saita, "The Change Of The Dynamic Characteristics Using Microtremor," in *The 14 th World Conference on Earthquake Engineering*, Beijing, China, October 12-17, 2008.

[11] B. Ş. ŞEKER, "Mimar Sinan Camilerinin Statik Ve Dinamik Yükler Etkisinde Davranışlarının İncelenmesi", Doktora Tezi, Trabzon: Karadeniz Teknik Üniversitesi Fen Bilimleri Enstitüsü, Ocak 2011. (in Turkish)